

Epidemic suppression via an emergent pre-conditioning field

T J Newman, SOLARAVUS

correspondence to: tjnewman@solaravus.com

Abstract

The COVID-19 pandemic is proving to be a severe test of current epidemiological and immunological frameworks and technologies. Several striking features have presented themselves, including the extreme disparity in infection and mortality rates from one country to another (and from one state to another within the US), the typically very slow decline of the epidemic after peaking in a given country, and the relatively low levels of infection in some countries (based on antibody testing) despite months of epidemic status. Clarity and consensus on the underlying reasons for these features is urgent in order to craft optimal strategies for ending lock-downs and planning for possible subsequent waves of COVID-19. In this paper we describe a framework that has the potential to explain these features of the pandemic. We hypothesise an emergent, long-ranged “pre-conditioning field” (PCF), generated by infected individuals and provoking a preliminary immune response in distant non-infected individuals. We show that incorporating a PCF within the simplest SIR model is capable of describing the epidemic features described above, and also predicts subsequent waves of epidemic if pre-conditioning deteriorates too rapidly over time. Long-ranged dispersal of viral detritus from infected individuals is discussed as a candidate mechanism for the PCF, and biophysical and immunological arguments are provided for its plausibility. Our main conclusions are relatively insensitive to the precise form of the PCF. Should the general concepts given here prove compelling, some proactive steps to tackle the pandemic within the PCF framework can be considered prior to a detailed specification of the PCF itself.

Contents:	<i>page number</i>
1. Introduction and motivation	3
2. The pre-conditioning field	5
3. Results from preliminary modelling	11
4. Summary and discussion	14
Appendix A: estimates of concentration of viral detritus	18
Appendix B: mathematical details	19
References	22
Acknowledgements	24
Short biography	
List of acronyms	
Supplementary information	
Figures	25

SOLARAVUS TECHNICAL REPORT

Report #: 003
Date: June 18th 2020
Title: Epidemic suppression via an emergent pre-conditioning field
Author: T J Newman

This is a technical report from the company SOLARAVUS and will remain freely available to all interested parties via the [SOLARAVUS website](#).

Note, given the universal interest in the current COVID-19 pandemic, this report is written with both scientists and the general public in mind as potential readers. An attempt has been made to minimise technical jargon, and to provide more comprehensive explanations of certain technical methods than would be usual in scientific articles appearing in journals.

If a citation to this report is required, please use reference number: STR 003 (a doi reference number will be obtained in due course).

1. Introduction and motivation

The COVID-19 pandemic originated in Wuhan, Hubei province, China in late 2019 (Zhu et al 2020), and has spread across the globe. COVID-19 is the disease caused by the SARS-CoV-2 virus (Bar-On et al 2020 and references therein). To date (June 2020) COVID-19 has infected well over 8 million people with a death toll in excess of 400,000 (*worldometers.info*). The pandemic has brought epidemiology into the spotlight as never before. Governments worldwide have urgently sought expert advice on how to weather the storm as COVID-19 sweeps through their nations, and the general public has become well-versed in principles such as “exponential growth”, “ R_0 ”, “herd immunity”, and “flattening the curve”. Detailed tracking of cases and mortality has been undertaken in many countries yielding rich datasets with which to evaluate conventional epidemiological and immunological models along with new theories.

Epidemiological modelling has been essential in providing early estimates of the infection and mortality rates of the disease (Kraemer et al 2020, Kucharski et al 2020, Lourenço et al 2020, Verity et al 2020, Wu JT et al 2020), and continues to be used to better understand the disease dynamics and to provide tools to evaluate lock-down strategies (e.g. Ianni and Rossi 2020, O’Sullivan et al 2020). A uniform consensus has yet to emerge about key aspects of the pandemic, despite similarities in modelling frameworks, with widely reported disagreements between epidemiologists on the timing and duration of the epidemic and the efficacy or otherwise of extraordinary government measures such as lock-downs. In addition, inverse modelling using Bayesian inference has concluded that very significant fractions of host populations may not be susceptible to the SARS-CoV-2 virus (Friston et al 2020, Moran et al 2020). This chimes with seroprevalence studies which show quite disparate rates of infection in countries that have experienced the infection for many months (Sereina et al 2020 and references therein, Streeck et al 2020). Additional striking features have emerged, such as the very significant disparity between mortality rates from one country to the next (and from one state to the next in the US) and the typically very sluggish decline of the epidemic after peaking in a given country (*worldometers.info*). To what degree these disparities are due to known factors (differences in efficacy of lock-downs, issues with accuracy of antibody testing, and genetic and immunological details of immune response (e.g. Wu F et al 2020)), or to fundamental gaps in our understanding of COVID-19 remains to be seen.

There is of course an urgency to better understand the pandemic that goes beyond scientific consensus. Societies and their elected representatives desperately need to determine the efficacy of various lock-down strategies, to optimise the rate of subsequent deregulation of social and economic interactions, and to better prepare for the next severe pandemic, which may indeed be a subsequent wave of COVID-19. As such, scientists, engineers, technologists and physicians, from a range of disciplines outside of epidemiology, have felt a moral and social imperative to employ their expertise to provide new ideas and innovations to governments, think-tanks and the epidemiology community. This paper is offered in this spirit, the ideas herein stemming from a theoretical biophysics perspective.

When confronting complex phenomena, particularly if conventional understanding is strained, there are two broad approaches to improve our understanding. The first might be termed “bottom up” where one uses existing knowledge and well-understood reductionist mechanisms in novel or more complex combinations in an attempt to describe the data. In the context of pandemic, this approach is evidenced by highly complex epidemiological models, in which dozens of demographic characteristics and detailed sociological and

geographical features are accounted for, to explain historical data and to predict the near and intermediate disease dynamics under various scenarios of government and healthcare interventions (Kenah et al 2011, Heesterbeek et al 2015, Chowell et al 2016, Lourenço et al 2020, Verity et al 2020). Such models will generally be able to fit historical data if enough modelling complexity is introduced. The second approach might be termed “top down” and in this case one seeks new hypotheses that can explain much of the data in a parsimonious manner, with little reliance on a large number of fitting parameters. Successful hypotheses might have, at first glance, tenuous connection to known mechanisms, but can lead to new understanding of the phenomena to hand. [An historical example of these two approaches in biology pertains to the classic problem of pattern formation during embryo development, with the first approach being realised through differential gene expression and regulation (Gilbert 2003), and the second through Alan Turing’s landmark paper on morphogen gradients (Turing 1952).] Each approach serves an important purpose to get to the heart of the matter, and over time are often seen to converge to a richer coherent understanding. This paper follows the spirit of the second approach of “top down” phenomenology, offering a new hypothesis which parsimoniously describes, qualitatively, much of the pandemic data, particularly the striking features described above, despite this hypothesis having from some perspectives less direct connections to known mechanisms.

In a recent interview oncologist Karol Sikora described epidemics ending “as if the virus gets bored” (Sikora, Unherd 2020). This phrase was vivid and clearly metaphorical, yet brought to the author’s mind a more intrinsic form of population response to epidemic, beyond behavioural responses such as social distancing. Could there be what one might call a superorganismal immunological response to a pathogen? Indeed, it is well known that bacterial and amoebal communities are capable of coherent population-level responses to environmental stress (Lewis 2007, Strassmann and Queller 2011) and so why not populations of more complex organisms such as humans?

This line of thought is consonant with the decades of work by Rupert Sheldrake and coworkers on morphic resonance – the idea that organisms within a species are capable of shared learning and behaviour through a hypothesised morphogenetic field that spans very large distances (Sheldrake 2009). The existence of morphic resonance remains controversial in the wider scientific community. Whilst Sheldrake’s concepts have inspired the hypothesis to be explored in this paper, our approach is not based on morphic resonance per se.

Our hypothesis is the following: that in a population experiencing epidemic there emerges a superorganismal immunological response. The mediator causally connecting the infected subpopulation with the remaining uninfected population is presumed to be long-ranged, providing protection beyond the region of the current infection, and we term it the “pre-conditioning field” (PCF).

In the next section we will describe how the PCF can be incorporated into the simplest epidemiological model, the SIR model (Bailey 1975) and we discuss qualitatively how it would affect the course of an epidemic. We will describe one possible instantiation of the PCF: large-scale dispersal of (non-live) viral detritus (ViDe) from infected individuals (Després et al 2012) carried by convective air currents over continental scales, and being subsequently inhaled by uninfected individuals, pre-conditioning their immune systems to later exposure to the live virus; an “early warning system” as it were. The conceptual and qualitative results of this paper, in particular given the overtly simple nature of the modelling, are relatively independent of the particular form of the PCF.

In section 3 we provide proof of principle by quantitatively investigating the effect of the PCF within the SIR model, using mathematical and numerical analysis. We show that the PCF is able to account for the striking features of the pandemic described above; namely, apparently low levels of seroprevalence, sluggish decline of the epidemic in a given region (the so-called heavy tail of the epidemic curve), and disparate rates of infection and mortality from one region to another (this, due to differing levels of pre-conditioning).

The paper ends with a summary of the main results. We discuss how one might test in more detail the validity and utility of the general idea of a PCF and the possibility that airborne ViDe is the relevant PCF in the COVID-19 pandemic. We discuss important real-world extensions of the SIR modelling framework to include the PCF. We also speculate on the evolutionary origins of the PCF and potential healthcare enhancements.

All mathematical details are to be found in the Appendices.

2. The pre-conditioning field

Conceptual definition of the PCF

Prior to discussing any particular instantiation of the pre-conditioning field (PCF), we aim to define it conceptually, and this can be accomplished most easily by considering how we would incorporate it into the simplest epidemiology model, i.e. the SIR model (black boxes and arrows in Figure 1). Following classical epidemiology (Kermack and McKendrick 1927, Bailey 1975) we disregard for simplicity all structure of a given population, e.g. age, gender, spatial distribution, and consider each individual to be in contact with all other individuals, and to belong to one of three categories or “compartments”, namely susceptible (S), infected (I) and recovered (R). [For the purposes of labelling interactions, we can aggregate deceased individuals with recovered individuals, since both are absorbing states in this simplest of models.] In the spirit of such models, transitions from one compartment to the next (e.g. S to I or I to R) are modelled using rate constants (i.e. processes with a constant probability of occurrence per unit time).

We illustrate the addition of a PCF to the SIR model with the blue boxes and arrows in Figure 1. The essential components are:

- i) the identification of a new category of individuals: “pre-conditioned” (P);
- ii) generation of the PCF by infected individuals;
- iii) a rate at which susceptible individuals, on exposure to the PCF, become pre-conditioned (note, this process competes with the infection transition S to I);
- iv) a rate for reversion from pre-conditioned back to susceptible;
- v) a rate (not illustrated) of degradation of the PCF through environmental processes.

This is essentially the simplest conceptualisation of the PCF, and in Section 3 (and Appendix 2) we provide a preliminary mathematical and numerical analysis of the corresponding mathematical representation of this model. We show that the PCF radically alters the dynamics of the SIR model, and we will see that it is straightforward to find combinations of rate constants that give epidemic trajectories qualitatively similar to those seen in COVID-19.

Intuiting the epidemic dynamics as a result of the PCF

Some of the main features of the effect of the PCF can be understood intuitively from the structure of the model, without the need for mathematics, as we now explain. If we first

ignore the reversion process we see that the pre-conditioned state is an “absorbing state”, just like recovery and death. In other words, once an individual enters that state they are removed from any subsequent processes. This means that pre-conditioning *competes* with infection for susceptible individuals. If the PCF is strong enough and the rate of pre-conditioning high enough, pre-conditioning will “win” this competition and claim more susceptibles than the infection process. In such a scenario, the PCF will have buffered the majority of the population from infection. Once all infected individuals have either recovered or died the epidemic will have completely ended with most individuals (those who are pre-conditioned) never having been infected. This simplest of all scenarios is reminiscent of ecological processes involving a refuge (Newman et al 2002, Berryman et al 2006), namely a location where individuals can shelter from population pressures (e.g. competition, predation or parasitism). What is unusual about this dynamics though is that the refuge is emergent; pre-conditioning is mediated by the PCF which is itself created by infected individuals. Thus, determining precisely how strong the PCF field needs to be to overwhelm the infection is non-trivial, as one needs to essentially solve for the entire epidemic dynamics in order to achieve this. In Appendix 2 we will provide an approximate solution of this problem by comparing the short-time growth trajectories of the infected, recovered and pre-conditioned populations.

Re-instating the process of reversion creates a richer set of possibilities for the epidemic dynamics. In this case, pre-conditioning is no longer an absorbing state – individuals who are pre-conditioned will eventually return to a susceptible state and are once again prone to infection. We will show from numerical solution of the model that a moderate level of reversion causes the epidemic to die away far more slowly. We can understand this as follows. At the start of the epidemic, as the number of infected individuals grows, the PCF grows proportionately. This triggers growth in the pre-conditioned population. If the PCF mechanism is strong, most of the susceptible individuals will become pre-conditioned and the rate of new infections will begin to wane. As this occurs, the PCF proportionately weakens. The process of reversion continually “drip-feeds” pre-conditioned individuals back into the pool of susceptibles. This then provides new material for the infection to “work on”, so to speak, and the decline of the infection rate will be reduced. This slows the decline of the PCF which in turn increases the net flux of susceptibles to a pre-conditioned state. We see how non-linear the epidemic becomes, as it slows down in this tug-of-war between infection and pre-conditioning mediated by reversion. The precise trajectory of the epidemic becomes too difficult to understand through intuition alone, requiring mathematics and/or numerical analysis.

In fact, as we shall see in section 3, by adjusting the rates of infection, pre-conditioning and reversion, the model exhibits more extravagant dynamics beyond drastic slowing of the epidemic decline. For a low rate of reversion new waves of epidemic are triggered from residual populations of infected individuals. These new waves can be understood from the discussion above – when the number of infected individuals becomes very small, the PCF will have all but vanished and over time the pre-conditioned population will revert back to susceptibles. This essentially mimics the start of the epidemic, albeit with a smaller susceptible population, and so long as there is a remaining pool of infected individuals new waves of epidemic will occur, each smaller than the last.

In principle one can fit the model presented here to the data of COVID-19 epidemic trajectories in various countries. We choose not to pursue that in this paper. In section 3 we will show qualitatively that the simplest model of PCF dynamics can reproduce key features of the pandemic. To go beyond this without accounting for very important real-world

features of the populations is of questionable relevance. The most important features to add are age structure, co-morbidities and gender – demographic characteristics driving much of the hospitalisation and morbidity data one would be attempting to fit (see for example COVID infection data for the UK at ons.gov.uk). Thus, fitting to real-world data is better explored by incorporating the PCF mechanism, as parsimoniously as possible, into existing population-structured epidemiological models.

Spatial dynamics of the PCF

The SIR model, when described in terms of compartments, dispenses with all spatial information. Nevertheless, the PCF is envisaged to act over long distances, whereas SARS-CoV-2 infection, as with many other diseases, is primarily transmitted by local contact (Bar-On et al 2020 and references therein). This spatial aspect of the PCF is illustrated schematically in Figure 2, and its ramifications can be intuitively explained as follows.

The epidemic starts in a well-defined region. All individuals bar the original rare infected individuals are susceptible. Infection spreads via local contact and the number of infected individuals increases exponentially. All infected individuals release an agent that contributes to the PCF. In the early stages of the epidemic, while the number of infected individuals is relatively small, the total PCF will be weak, but growing exponentially.

Over time, the number of infected individuals continues to increase by local contact interactions and the region of epidemic spreads (red region in Figure 2). The concentration of the PCF increases proportionately and, via long-range spreading, interacts with more distant populations which have yet to experience any infections. These more distant populations become increasingly pre-conditioned by the PCF (blue region in Figure 2). The epidemic is subsequently expected to be less severe in the mainly pre-conditioned populations, in terms of transmissibility, severity, infection rates and mortality rates.

Spatial transport or spreading of the PCF is not instantaneous, and so there will be very distant populations which are “naïve”, neither experiencing the infection nor the PCF. In this modern age of intercontinental air travel the infection can be rapidly transported to these naïve populations, seeding new epicentres of epidemic. In these regions with no pre-conditioning the early spread of the disease will mimic the original epidemic, with higher transmissibility, severity, infection rates and mortality. Over time, these new epidemics will create their own spreading PCF giving protection to adjacent populations.

This intuitive narrative of the spatial aspects of the PCF mechanism has a degree of consonance with some of the continental-scale aspects of the pandemic:

- i) the rapid spread and high initial mortality rates in the COVID-19 epicentre of Wuhan (Wu JT et al 2020, Verity et al 2020);
- ii) the apparently less aggressive dynamics of COVID-19 in some geographically adjacent regions (e.g. Japan, Australasia, SE Asia, Eastern Europe) ([worldometers.info](https://www.worldometers.info))
- iii) the high infectivity and mortality rates seen in those regions geographically farthest from the original epicentre (e.g. US eastern seaboard, and parts of S America) ([worldometers.info](https://www.worldometers.info))

At this time, these are little more than intriguing qualitative observations, and may well be explicable in terms of national differences in lock-down strategies, population density, population structure, etc. If the PCF is responsible, then identification and characterisation of the underlying PCF mechanism is necessary in order to quantify its rate of spatial spreading and its subsequent effect on geographical differences in disease severity.

An instantiation of the PCF – viral detritus

It is helpful then to attempt to be more specific in envisaging the PCF. As mentioned in section 1, the original conception of the PCF is that of a superorganismal response, and was inspired by the work of Rupert Sheldrake on a morphogenetic field that allows all organisms of a particular species to share learning and new behaviours over arbitrarily long distances via morphic resonance (Sheldrake 2009). These concepts remain controversial, yet provide a helpful starting point in conceptualising the nature of the PCF and seeking instantiations based on more broadly accepted scientific principles.

The instantiation we consider here, particularly pertinent to COVID-19 and other respiratory illnesses, is that the PCF is a concentration field of viral and immune system fragments, which we denote collectively as “viral detritus” (ViDe). ViDe from fragmented SARS-CoV-2 viruses, along with live virus particles, is emitted into the surrounding air by infected individuals through breathing and coughing. We must be clear at the outset to distinguish long-range transport of ViDe from short-range transport of live virus. The long-range transport of all manner of biological agents (collectively known as bioaerosols), whether they be fungal spores, bacteria or viruses, is well-documented (Després et al 2012), though it is recognised that viruses have very low survivability outside the host. Indeed, studies have shown that the live SARS-CoV-2 virus is transmitted locally, through inhalation of locally exhaled microscopic water droplets containing the virus, or through contact with recently exposed surfaces, but is unlikely to survive in live (infectious) form over longer distances and timescales (Bar-On et al 2020 and references therein). Thus, in discussing the PCF we are not concerned with the survival of the live virus, but rather with long-ranged spatio-temporal dispersal of fragments of the virus, be it RNA, capsid fragments or individual capsid protein molecules, a significant proportion of which we assume to remain structurally intact in air currents over significant time periods.

To determine whether it is plausible that ViDe can be transmitted over long distances in detectable concentrations, it is helpful to first consider a well-known paradigm about the non-intuitive nature of such questions. One asks the following odd question “each time an individual in 2020 breathes, how many molecules do they inhale from the final exhalation of Julius Caesar on his death on March 15th 44 BC?” At first glance the question seems bizarre but is worth investigating as the answer is surprising and informative. It turns out that every time we breath we inhale on average one or two molecules from Caesar’s last breath. The calculation is presented in the first part of Appendix A. It is a beautiful example that highlights how our intuition can be misleading when trying to marry the product of a very large number (the number of air molecules in Caesar’s last breath) and a very small number (the ratio of the volume of Caesar’s last breath to the volume of the Earth’s atmosphere). It is this breakdown of intuition in the Caesar paradigm that we believe may lend an unexpected plausibility to ViDe acting as a PCF.

In the second part of Appendix A we provide a parallel analysis of ViDe, in the spirit of the Caesar paradigm. Crude estimates are by necessity used, and so the outcome can only be determined to within a few orders of magnitude at best. We estimate that an individual infected with SARS-CoV-2 exhales a total of ca 10^{14} molecular viral fragments over the course of their illness (note, we do not distinguish between clustered molecules constituting fragments of virus particles or completely disassociated molecules/complexes). This number may seem large at first, but to put it into perspective, consider the following: each human breath contains ca 10^{22} air molecules, and so 10^{14} viral fragments (where each biomolecule has a mass of ca 10^5 daltons, and where this number is the total over the 5-10 day course of the illness) has one ten thousandth of the mass of air exhaled in a single breath. Following

the Caesar paradigm, we then estimate that subsequent to the first phase of the COVID-19 pandemic, when the cumulative number of infected individuals reached of order 1 million (including both mild and severe cases), susceptible individuals in distant regions from the epicentre will subsequently be inhaling, *on average*, ca 1 molecular SARS-CoV-2 fragment per minute (which scales up to ca 1000 fragments per day, or ca 50,000 fragments in one month). These numbers are not negligible, and thus provide a degree of plausibility to the idea that ViDe can act as a PCF over continental and global length scales.

Crucially, the estimate of ViDe concentrations is averaged in the sense of assuming that ViDe is completely mixed in the Earth's lower atmosphere with a uniform concentration over the entire surface of the Earth. This will not be the case over the relatively short timescales of the pandemic, namely weeks and months. Lack of statistical atmospheric mixing across the entire globe over these shorter timescales will mean that the concentration of ViDe will be orders of magnitude higher in some locations, directly downstream of air currents emanating from COVID-19 epicentres, and orders of magnitude smaller in regions which are quiescent in terms of such convective transport. Thus, within the PCF hypothesis, some regions of the world would benefit from strong pre-conditioning and would thus experience milder epidemics, whilst others would have little if any preconditioning and would thus experience the full onslaught of the epidemic in the manner of the original epicentre in Wuhan. To give further plausibility to the ViDe mechanism of pre-conditioning it will be essential to analyse global air currents over the period January to June 2020, seeking correlations between convective transport patterns emanating from infection epicentres and disease severity in downstream areas (higher flux of air currents via convective transport from the epicentre giving higher PCF and thus lower subsequent disease severity, and *vice versa*).

We stress again that the estimates given above are unavoidably very crude. If ViDe is determined to be a plausible instantiation of the PCF concept, there will be a need for in-depth interdisciplinary research, involving immunologists, virologists and atmospheric scientists, to provide more accurate (or, one might say, less inaccurate) estimates of ViDe concentrations. We refer the reader to a recent comprehensive summary of airborne disease transmission from the Lawrence Livermore National Laboratory (Dillon and Dillon 2020), which demonstrates the complexity of spatio-temporal particle dispersion over local, regional, and continental scales.

One can also consider the effect of pre-conditioning from ViDe at smaller scales. There will be higher levels of ViDe in densely populated areas, such as large metropolitan areas, during the period of highest infection, and although this ViDe will disperse beyond the area relatively quickly, it will for a short period be at far higher concentrations locally than calculated for average global levels. Likewise, ViDe will be present at very high concentrations in the homes of infected individuals, and may provide pre-conditioning and protection to other members of households assuming that high levels of hygiene are followed that delay immediate contact infection. This chimes with the recent surprising finding of low rates of secondary COVID-19 infections in homes (Streeck et al 2020).

Immunology and the PCF

A critical component of the PCF mechanism is, of course, the response of a susceptible individual's immune system to the pre-conditioning field. If the PCF is a concentration field of ViDe, the physiological question is: can fragments of virus pre-condition the immune system to later exposure to live virus, and if yes, can this occur through inhalation, and how does it depend on concentration and types of fragments? Only immunologists can give

precise answers to these questions, bearing in mind the extraordinary complexity of the immune system and the fact it remains one of the most active areas of discovery in biology. Vaccination works in a not dissimilar fashion to that envisaged for the PCF, using either related viruses or deactivated viruses to trigger an immune reaction giving subsequent long-lived protection from a specific viral pathogen. Vaccination is typically discussed in terms of triggering the adaptive immune system, thereby raising antibodies and establishing a population of memory T cells, available to rapidly mount a full immune response on later exposure to the live virus (Sallusto et al 2010). However, it is well known that vaccines elicit far broader responses in the host, including long-lasting changes to the innate immune system (Kleinnijenhuis et al 2012, Benn et al 2013). We therefore envisage the ViDe instantiation of the PCF as an emergent, low specificity, low concentration vaccination. Emergent, as it is created by the disease itself through the exhalations of ViDe from infected individuals; low specificity since the ViDe will be a “soup” of various viral (and possibly immune system) fragments; low concentration because of the nature of the mechanism, as has been described in some detail above. We note also the phenomenon of “ischemic preconditioning” (McDonough and Weinstein 2016), in which long-lasting immunological buffering against severe outcomes of stroke is provoked by a brief period of cerebral ischemia, and mediated by innate immune response pathways. This clinical finding illustrates that immunological preconditioning can take unusual, even counter-intuitive forms, encouraging us to be catholic in our thinking about putative instantiations for the PCF, should it indeed exist.

For pre-conditioning to be effective the immune system needs to be highly sensitive to incoming signals – both biochemical (e.g. ViDe) as well as biological (e.g. live viruses). We know this is possible in principle from the everyday experience of allergic reactions: overactive immune responses to low concentrations of both chemicals (e.g. perfumes) and non-pathogenic foreign bodies (e.g. dust mites, pollen grains). In section 4 we will return to this point more generally and argue for high levels of sensitivity based on biological analogues and evolutionary principles. One specific point we can make here relates to the composition of the ViDe for SARS-CoV-2. Coronaviruses are so called because of their halo appearance under the microscope, which is caused by the viral envelope being studded by so-called “spike trimer complexes” (Bar-On et al 2020 and references therein). Indeed, it is these spike proteins that allow the virus to firmly attach to cells in the lung epithelium and mucosal tissues, thereafter provoking endocytosis and infecting cells. A significant proportion of the ViDe will comprise spike proteins (each original virus particle contains ca 100 spike trimer complexes). On inhalation of ViDe by a susceptible individual it would appear plausible that spike proteins can still attach to cells in the lung epithelium. This will be harmless as the proteins are not attached to live virus. Nevertheless, this could presumably cause a low-level lasting immune response in the host (either innate or adaptive, as discussed above), particularly if individuals have previously experienced infection of related coronaviruses. One last point concerns the dependence of an individual’s PCF response on characteristics such as gender, age and pre-existing conditions. For example, the elderly, with weaker immune responses, would experience a “double hit”, receiving less benefit from pre-conditioning and being more prone to severe infection. Similar “double hits” would be an issue in immuno-compromised individuals. As such, strategies on exploiting pre-conditioning would need to account for such characteristics.

Thus, ViDe appears to have a sufficient degree of plausibility to warrant further study as a candidate for the mechanism of pre-conditioning in SARS-CoV-2. We turn now to a mathematical and numerical analysis to demonstrate that in its simplest possible form the PCF mechanism reproduces key dynamical features of the COVID-19 pandemic.

3. Results from preliminary modelling

Modelling principles

As we saw in the previous section, given the strongly non-linear, emergent nature of the PCF, it is not possible to use purely intuitive arguments to understand the full dynamics of an epidemic in the presence of a PCF. For this reason it is necessary to use mathematics, numerical analysis and/or simulations to obtain a quantitative understanding, along with predictions that can then be tested against real-world data. Comparison of the model against data allows an evaluation of the validity of the PCF hypothesis – does it provide a parsimonious description of the COVID-19 pandemic and other epidemics?, does it need fundamental refinements?, or is it plain wrong and of no use? In this section we provide a first step towards such a comparison, namely a proof of principle test, by analysing the simplest possible mathematical instantiation of the PCF. We will find that the PCF mechanism passes this test, and is able to reproduce key qualitative features of the epidemic dynamics without fine tuning of parameters.

Given this preliminary model is so simple, we will not attempt to fit model parameters to real-world data. Two important issues forbidding this are: i) the intrinsic variation from one country to the next in how data is collected, particularly the absence in the data of the number of infected individuals, as generally only severe cases are tracked, and ii) the importance of key demographic characteristics, particularly age, gender and pre-existing conditions. The proportions of individuals with these characteristics in the susceptible population will have very strong effects on the numbers of severe cases and mortalities, and so any model that attempts to fit data in a meaningful way must include sub-population structure representing these characteristics. These added layers of sophistication take us beyond the scope of this preliminary analysis. Detailed subpopulation models exist in the epidemiological community, as discussed in section 1, and it will be possible, should there be sufficient interest, to incorporate the PCF mechanism described here into those models, and then to perform systematic fitting to data.

We refer the reader to Appendix B for a description of the classic SIR epidemic model and how the PCF can be straightforwardly incorporated into this framework, resulting in the boxed set of five coupled differential equations. We list below the parameters of the model (all of which are rate constants), as we will refer to their values in subsequent discussion and figures. We use a convention whereby variables describing the subpopulation densities (but not the PCF) are denoted by Roman letters, and parameters are denoted by Greek letters.

α – rate at which a susceptible individual is pre-conditioned on contact with the PCF

β – rate of infection given contact between susceptible and infected individuals

γ – rate of leaving the infected state (the sum of recovery and death)

ε – rate at which a pre-conditioned individual reverts to being susceptible to infection

κ – rate of production of the PCF by infected individuals

λ – rate of environmental degradation of PCF

It might seem odd that we do not distinguish between recovery and death, instead combining them in the parameter γ . In this simplest model, individuals who have left the infected state, whether through recovery or death, play no further role in the epidemic dynamics. Given our interest is in the epidemic trajectory, there is no need mathematically to distinguish them. Of course, if one is fitting a more detailed model to infection/mortality data, then it will be necessary to separately track these different outcomes from infection.

One further comment on the structural formulation of the model is in order. One might argue that pre-conditioned individuals are still liable to infection, just less so than susceptible individuals. This would seem to be quite reasonable, and a more sophisticated model might have “degree of pre-conditioning” as a continuous variable within a susceptible compartment. In the interests of simplicity we are imposing here a bi-modal distribution on pre-conditioning, so that an individual is either not pre-conditioned, and is hence susceptible, or is entirely pre-conditioned, and is hence not liable to infection whilst in that state, though can revert back to being susceptible over time.

In the analysis below, we first look at the behaviour of the model in the absence of reversion ($\varepsilon = 0$). This enables us to understand most straightforwardly how pre-conditioning can buffer the population from infection. The dynamics of the epidemic in this case are relatively simple. We then introduce reversion ($\varepsilon \neq 0$) and find a richer set of epidemic dynamics, including “heavy tails” in the epidemic curve and spontaneous multiple waves of epidemic.

The strong non-linearities in the set of differential equations forbid a direct mathematical solution of the entire epidemic trajectory. As such, numerical analysis is the main method to understand the model. We use a computer algorithm to integrate the differential equations forward in time for given values of the parameters – this allows us to study detailed epidemic trajectories, and we can explore the range of such trajectories by varying the parameters. Because there are six rate constants in even this simplest of models, the “parameter space” is in fact quite large, and we do not attempt to explore it exhaustively in this preliminary analysis. Instead, guided by intuition, we investigate particular regions of parameter space and demonstrate that the model robustly (meaning without fine-tuning of parameters) reproduces key qualitative features of the epidemic. The code for the computer algorithm is provided as a supplementary file so that all interested parties can investigate the model and extend it as they see fit.

No reversion ($\varepsilon = 0$)

We provide in Appendix B an approximate mathematical solution for short times under the simplifying condition of no reversion. This is useful as it shows that pre-conditioning can dominate over infection and recovery, even though the PCF depends on infected individuals for its very existence. The analysis gives the following approximate condition on the rate constants for pre-conditioning to be dominant: $\alpha\kappa > \beta(\beta - \gamma + \lambda)$. Numerical solutions show that this bound is in fact too stringent, and that lower strengths of PCF are still sufficient to dominate the dynamics. The important qualitative point is that pre-conditioning can act as a buffer for the majority of the population against infection, regardless of the rates of infection and PCF degradation, so long as the rates of PCF production and pre-conditioning are sufficiently high.

Buffering is confirmed through numerical integration of the SIR model with the additional PCF mechanism (the boxed differential equations in Appendix B). The panels in Figure 3 show the densities of the subpopulation compartments as a function of time, with the total population density normalised to unity. The PCF mechanism is gradually increased in strength from zero in panel A to increasing values across panels B to D (we keep all other parameter values fixed and successively increase the value of α). Details of initial conditions and parameter values are given in the figure caption. As the rate of pre-conditioning is increased the susceptible population (green) is increasingly channelled into a pre-conditioned population (orange), and is thereby buffered from the infection (red). Note, this pre-conditioning is emergent – arising from the PCF which is itself generated from the infected population.

This is a primary result of the PCF mechanism. It shows that if pre-conditioning is occurring during the epidemic then a significant section of the population will never have been infected. This provides a possible explanation to a number of recent reports from different countries who find relatively low proportions of the population with antibodies to SARS-CoV-2 despite the population having passed the peak of the epidemic trajectory (Sereina et al 2020 and references therein). It also chimes with recent work (Moran et al 2020) using Bayesian inference to determine underlying variables driving the epidemic dynamics in the UK and several other countries. The study revealed that epidemic trajectories could be best explained if susceptible populations were many times smaller than total populations. The PCF explanation of this finding is universal across countries, in that the buffering of the susceptible population is an emergent phenomenon of the epidemic itself, requiring no specific heterogeneities in the genetics, diets or lifestyles comprising the population.

Including reversion ($\varepsilon \neq 0$)

It is unlikely that the pre-conditioned state is permanent for a given individual. This would presumably require a strong, specific adaptive immune response raising antibodies and creating memory T cells, and is at odds with much of the seroprevalence data as discussed above. Therefore, it is important to consider the effect of reversion, by which we mean the process of a pre-conditioned individual once again becoming susceptible and open to infection. [In the earlier discussion of ViDe as a candidate for the PCF, we discussed its effect as akin to that of a low-specificity vaccine, eliciting an innate immune response, and it may be that such responses decay fairly rapidly, over time-scales of weeks or months, unlike the potentially life-long protection given by memory T-cells after an adaptive immune response.]

The panels of Figure 4 show numerical integration of the SIR model with the additional PCF mechanism, but now varying the rate of reversion ε . Panels on the left show the densities of the subpopulations as a function of time. Partner panels on the right are for the same parameter values and show the rate of increase in “recovered” individuals, which we define as the epidemic curve and denote by $q(t)$. It is one measure of the “shape of the epidemic” giving periodic (e.g. daily) values for newly recovered (and/or deceased) individuals. The figure caption gives details of initial conditions and parameter values. [Note the change in y-axis scaling in the right-hand panels.] The twin panels A correspond to an extremely high value of reversion $\varepsilon = 10.0$, and is included purely as a check, to confirm intuition. In this case pre-conditioned individuals almost immediately revert back to being susceptible and as such the PCF is almost completely ineffective at buffering the population. Note in this case that the epidemic curve $q(t)$ rises rapidly and decays equally rapidly.

The twin panels B correspond to a reversion rate $\varepsilon = 0.08$, which is of the same order of magnitude as the values of other rate constants in the model, and less than the infection and pre-conditioning rates. In this case we observe a very interesting effect: the right tail of the epidemic curve $q(t)$ decays very slowly – giving what is called a “heavy tail” of the distribution. This has been observed in many countries (*worldometers.info*). This analysis shows that heavy tails are a straightforward outcome of the hypothesised pre-conditioning mechanism, thereby lending support for the hypothesis. It is likely that more realistic metapopulation models, or spatially explicit models, will generate even more slowly decaying tails of the epidemic curve, through desynchronisation effects.

In twin panels C, we show the results of reducing the reversion rate still further to $\varepsilon = 0.01$. Here we see a new effect, namely repeated waves of epidemic. This is entirely intrinsic to the emergent properties of the system. It arises because when the reversion rate is very low,

pre-conditioned individuals are returned to the susceptible compartment quite late in the epidemic, but before the infection has completely died. This essentially restarts the epidemic anew, though with a smaller total number of susceptibles. Successive waves can be seen, each smaller than the last. In a more realistic model the epidemic would finally end if the density of the infected compartment between epidemic waves was smaller than the equivalent of one individual.

Finally, in twin panels D reversion has been completely removed, and we return to the type of behaviour seen in Figure 3 – very strong buffering of the population and suppression of the epidemic. Note the symmetric shape of the epidemic curve in D2. This indicates that, given the frequent occurrence of heavy tails in the real-world data, reversion is likely to be an essential ingredient for the application of the PCF mechanism to the COVID-19 pandemic. The effect of buffering is still present in this case, but far more dynamic.

In summary, preliminary numerical integration of the very simplest model of PCF dynamics shows many interesting features which mirror those observed in the actual epidemic data across many countries. No parameter fine-tuning has been required as these behaviours appear to be robust emergent properties of the model. It is hoped that this promising preliminary analysis will convince epidemiology groups to incorporate the PCF mechanism into more realistic epidemic models to better determine, through fitting to data, whether it provides a parsimonious understanding of epidemic data across multiple countries.

4. Summary and discussion

The PCF hypothesis

In this paper we have investigated the hypothesis of a “pre-conditioning field” (PCF) to explain various features of the COVID-19 pandemic. The PCF is conjectured to be a long-range field generated by infected individuals and providing immunological pre-conditioning to susceptible individuals (both in the vicinity of and distant from infected populations). Fundamental to this hypothesis is the notion that the PCF is an emergent outcome of the infection itself – a superorganismal immunological response.

Summary of results and next steps for modelling

In section 2 we described the PCF within the context of the simplest epidemiological framework, the SIR model (Bailey 1975). We used intuitive reasoning to understand how the PCF will influence the epidemic dynamics, the outcomes of which were subsequently confirmed by a preliminary mathematical and numerical analysis of the model in section 3, as summarised below. We used similar reasoning to describe the spatial influence of the PCF – providing buffering of populations distant from the epidemic over time, whilst still leaving very distant “naïve” populations unbuffered over shorter timespans, and thus vulnerable to severe epidemic outbreaks due to intercontinental air travel of infected individuals. We discussed how this was consonant, at first glance, with some aspects of the large-scale continental impact of the COVID-19 pandemic, with regions closer to the Wuhan epicentre being less badly affected (e.g. Japan, Eastern Europe and Australasia) than those on the opposite side of the globe (e.g. Brazil and the US eastern seaboard) (*worldometers.info*).

We discussed in some detail one possible instantiation of the PCF, relevant to COVID-19 (and other influenza type illnesses), that being a concentration field of viral detritus (ViDe). We provided (necessarily crude) order of magnitude estimates to inform the plausibility of this

mechanism of pre-conditioning, drawing on the well-known Caesar paradigm of long-range transport of air molecules around the globe. We estimated that in the early stage of the pandemic, with approximately 1 million people infected, the ViDe field would, on average, lead to each person on Earth inhaling one molecular fragment of the SARS-CoV-2 virus every ten breaths, which corresponds to approximately 50,000 inhaled fragments per month. We discussed immunological aspects of response to PCF, likening it to an emergent, low specificity, low concentration vaccination. We discussed briefly the non-specific effects of vaccines on both the innate and the adaptive immune systems, and that spike proteins, as a key component of the SARS-CoV-2 ViDe, could possibly bind to cells in uninfected individuals and thereby trigger a low-level pre-conditioning immune response.

In section 3 we used mathematical and numerical analysis to explore the influence of the PCF on epidemic dynamics using the SIR model as a framework. We found that this simple model was able to reproduce many of the features of the COVID-19 pandemic: the possible large-scale buffering of populations in the presence of the infection and the slowly decaying “heavy tail” of epidemic curves (and, for other choices of parameters, a sequence of recurring waves of epidemic). The PCF provides a universal and emergent resolution of the recent finding from Bayesian inference studies, that the pandemic dynamics are best explained by the susceptible populations being much smaller than the actual populations (Moran et al 2020). Despite the highly non-linear nature of the PCF mechanism, these features are intuitively comprehensible from considering the competition between infection and pre-conditioning processes for susceptible individuals, with the peculiar feature that the PCF requires infected individuals for its very existence. It is this “tug-of-war” between infection and pre-conditioning, with a drip-feed of new susceptibles from the pre-conditioned population through reversion, that yields the behaviours of dynamic buffering, slowly decaying epidemic tails and repeated waves of epidemic (seen in different regions of the parameter space of the rate constants controlling the underlying processes).

This analysis constitutes important proof of principle for the PCF as a parsimonious explanation of many features of the COVID-19 pandemic dynamics. The SIR/PCF framework (in its simplest form given by the boxed equations in Appendix B) is not limited to any particular instantiation of the PCF, such as ViDe. If there is sufficient interest from the community, it would be interesting to see if the inclusion of the PCF into more realistic model frameworks can yield similarly parsimonious, robust explanations of real-world data. We have argued that fitting of the PCF mechanism to real-world data is best done in models that at least capture the critical demographic categories of age, gender and pre-existing conditions, given the extremely high sensitivity of outcomes related to these categories (e.g. COVID-19 mortality data from England and Wales, ons.gov.uk).

Indeed, more sophisticated modelling will be essential when considering particular instantiations of the PCF. Particularly important in this regard is the inclusion of spatially explicit dynamics. A range of such models has been developed, many for influenza type epidemics (Viboud et al 2006, Bedford et al 2010, Kenah et al 2011). Such models do not generally consider biophysical processes, such as large-scale air currents. Should the ViDe instantiation of the PCF be considered plausible, these models in conjunction with detailed analysis of continental-scale air currents in early 2020 can be used to test for a correlation between high flow rates from infected regions and lower rates of infections and mortality in downstream regions (higher transport of ViDe into a region leading to stronger pre-conditioning and thus better outcomes during the epidemic dynamics in that region, and *vice versa*).

The top-down philosophy of PCF and its evolutionary context

As discussed in section 1, the PCF is offered as a top-down hypothesis. If the general PCF mechanism is able to explain a significant amount of data without fine-tuning then there is good reason to believe that it is capturing the effects of hitherto unidentified lower-level processes that can then be investigated in more detail. This approach is in the spirit of Turing's landmark paper hypothesising morphogen gradients of activators and inhibitors to explain pattern formation in embryogenesis (Turing 1952). His work, in tandem with intensive bottom-up investigations using developmental genetics (Gilbert 2003), has led to a richer and more coherent understanding of embryo development. There are many other examples of the success of this dual approach in science (throughout physics and chemistry, and also in ecology and evolution). In the modern era, particularly in biology and medicine, there is perhaps an unduly strong preference for bottom-up molecular mechanisms as the "gold standard" or even the "only standard". This can be self-limiting, particularly in terms of innovations for improving public health.

The most successful top-down theory in biology is Darwin's theory of evolution by natural selection (Darwin 1859, Mayr 2000), and it is interesting to consider the PCF from an evolutionary perspective. If the PCF mechanism exists, it might be described as an "emergent superorganismal immunological response". This is reminiscent of superorganismal behaviours in other populations, e.g.

- i) dormancy strategies in bacterial colonies under environmental stress, with a fixed concentration of persisters arising in the population through successive rounds of challenge (Lewis 2007);
- ii) the collective migration and sporifying strategy of *Dictyostelium* amoeba under starvation conditions, using a chemotaxis signalling field to cohere population-level behaviour, including self-sacrifice and altruism (Strassmann and Queller 2009);
- iii) the life cycles and natural histories of social insects, much of which relies on population responses through pheromone signalling (Wilson EO and Hölldobler 1990);
- iv) the long list of herding and swarming strategies in various animal groups to mitigate predation pressures (Parrish et al 2002, Ballerini et al 2008).

We often think of population-level behaviours of humans arising from sociological interactions rather than deeper innately biological ones. The existence of such biological behaviours, and their evolutionary significance, has been a matter of intense debate for decades (see e.g. Wilson 1975, Sheldrake 2009). Thinking of the PCF in these terms, one can frame the question: if a population-level immunological response is possible in humans, would evolution through natural selection having found it then dispense with it? In other words, is fitness in the face of pandemic improved by discarding an altruistic (population-level) immune response and relying exclusively on "selfish" (individual-level) ones, namely the well-studied innate and adaptive immune systems each of us possesses? Although human populations are genotypically diverse, each individual would benefit from a population-level response to a new pathogen, including those individuals spatially co-located with infected individuals, who would tend to be more genetically related. The individual immune response still provides natural selection with "grist for the mill" for selection pressure at the individual level. On this basis one sees little reason *a priori* why evolution would deselect superorganismal immunological responses.

The PCF is in fact quite a primitive strategy when viewed in these terms. It is not using the total antibody library of the population to find a cure-all. It is more of an early-warning system, buffering the population from infection; akin to an emergent (naturally-produced),

broad-spectrum vaccination. Indeed, we have discussed in some detail the ViDe instantiation of the PCF, which would allow population-level pre-conditioning for all manner of viral diseases which utilise airborne transmission. Admittedly, the concentration of ViDe is very small – we estimated 1000 fragments per day inhaled on average by each person on Earth through ViDe produced by a cohort of one million infected individuals. This requires tremendous sensitivity of the immune system; acting like a radio telescope, receiving all manner of very weak signals, and being able to refine signal from noise. But then, in defense of this idea, extraordinary sensitivity and exquisite filtering are in fact typical outcomes of evolutionary processes, and common in humans, e.g. the sensitivity of the human eye to light levels in the few photon range (Tinsley et al 2016) and the filtering ability of humans to instantly recognise familiar faces in a crowd (Chang and Tsai 2017).

Is there then more to breathing than meets the eye? Beyond fulfilling our need for oxygen, is it also a mechanism, mediated by ViDe, connecting individual immune systems and allowing pre-conditioning to airborne diseases at the population scale? Perhaps the cough response of flus and colds is not an evolutionary innovation of the virus to spread infection, but, in fact, an innovation from the host population to spread pre-conditioning.

PCF and the COVID-19 pandemic

This paper is being completed in mid-June 2020. The pandemic is very slowly dying down in Europe, Asia and the US, but rages in other parts of the world (*worldometers.info*). Many countries are tentatively relaxing lock-down regulations, but there is a climate of fear and uncertainty about recurrence of the epidemic and subsequent future waves. There is talk of “a new normal” of long-term enforced social distancing.

If the PCF concept has some level of validity it will provide insights to help interpret epidemic data and to optimise future strategies, lessening the need for lock-downs and social distancing, with all of their consequent deleterious effects (e.g. under-treatment of other illnesses, less effective education delivery, economic decline, exacerbation of mental health conditions, and restrictions on personal liberty). The level of pre-conditioning in each population can be estimated from epidemic data and used as a guide to predict the degree of buffering each population has to new waves of the epidemic. The preliminary modelling in this paper shows that reversion of the pre-conditioned state makes buffering more dynamic, slows the decline of the epidemic and spontaneously triggers new waves. Thus, with the caveat that *if* the PCF concept has some degree of validity, key interventions would be to enhance the level of pre-conditioning and/or to slow the rate of reversion. This is particularly important for the elderly and the immuno-compromised, who are likely to be less sensitive to an ambient PCF, on top of having elevated risk of severe illness should they become infected. If ViDe is confirmed as the mechanism underpinning the PCF, then (with tongue slightly in cheek) we can envisage wind-farms, not harvesting energy, but pumping out ViDe of the latest flu strain or head cold. We can envisage encouraging individuals to cough more – not near others, but far enough upstream that water droplets containing live virus are safely grounded whereas viral fragments are widely dispersed.

On a final forward-looking note, we can take advantage of the detailed data arising from the COVID-19 pandemic, and the resulting conundrums presented to both the scientific community and the general public, to take stock of our current immunological and epidemiological understanding. There is opportunity in challenge. Combining top-down and bottom-up approaches may identify fundamental new concepts with the potential to transform medical interventions in the treatment of infectious disease.

Appendix A: estimates of concentration of viral detritus

The Caesar paradigm

Consider the air molecules exhaled in the final dying breath of Julius Caesar on that fateful day in March, 44 BC. How many of these molecules on average do we each inhale with each breath? We can use straightforward order of magnitude estimates to determine this. The average tidal volume (breath) of a human adult is 0.5 litres (Saladin 2007). One mole of air contains Avogadro's number (ca 6×10^{23}) of molecules and occupies a volume of ca 20 litres at STP. Thus, one tidal breath contains ca $(0.5/20) \times 6 \times 10^{23} \sim 10^{22}$ air molecules. Caesar is chosen for this paradigm because he is a clearly identifiable figure from ancient history – enough time has passed that the molecules from his last breath have fully mixed with the air in the Earth's atmosphere, i.e. "Caesar's molecules" are statistically uniformly spread in the atmosphere. Next we estimate the volume of air in the Earth's atmosphere. The surface area of the Earth is $4\pi r^2$ where r is the Earth's radius, which has the approximate value 6000 km, or 6×10^6 m. The density of air decreases exponentially with height in the atmosphere, so we take the height of the lowest atmospheric layer (the troposphere) as an estimate, and that is ca 10 km, or 10^4 m. Thus, the volume of air in the Earth's lower atmosphere is ca $4\pi \times 36 \times 10^{12} \times 10^4 \text{ m}^3 \sim 5 \times 10^{18} \text{ m}^3$. One cubic metre is 1000 litres, and thus 2000 tidal volumes, and so the volume of air in the Earth's lower atmosphere is ca 10^{22} tidal volumes (breaths). Therefore we have the remarkable result that the relative volume occupied by one air molecule at STP to the volume of a human breath is the same as the relative volume of one human breath to that of the entirety of air in the Earth's atmosphere. Thus, given the molecules from Caesar's last breath are well mixed in today's atmosphere, we, each of us, with each breath, inhale on average one molecule of Caesar's last breath.

Average concentrations of viral detritus

(specific data on coronaviruses including SARS-CoV-2 is from Bar-On et al 2020 and references therein; subsequent percentage estimates are those of the author)

We can attempt a similar analysis to estimate the amount of viral detritus (ViDe) in the Earth's atmosphere arising from a population of infected individuals, and to then determine the amount of ViDe inhaled by distant individuals. The estimates used here are necessarily very crude. Some of the data required on SARS-CoV-2 is the subject of current research, but previous research on coronaviruses allows informed estimates. A typical infected individual will have viruses replicating in pneumocytes and alveolar macrophages in the lung and in cells lining the mucosal membranes. The number of cells in these tissues ranges from 10^9 to 10^{11} . Assuming a 10% cell infection rate over the course of the illness, we take ca 10^{10} as the number of infected cells. SARS-CoV-2 viruses bud off from the host cell, and it is estimated that infected cells each create ca 10^3 viruses. Each virus comprises various protein molecules (in the capsid and spike trimer complexes) and the viral RNA genome. The number of such constituent molecules is ca 10^3 . Assuming that 10% of viruses (or their constituent fragments) are exhaled by the infected individual, and that 10% of these fragments remain intact in the atmosphere, we estimate that an infected person over the course of their illness exhales ca $10^{10} \times 10^3 \times 10^3 \times 10^{-1} \times 10^{-1} \sim 10^{14}$ intact molecular viral fragments into the atmosphere. Thus, an infected population of 1 million individuals will release ca 10^{20} viral fragments into the atmosphere. Since these fragments are significantly more massive than air molecules, we assume that they are mainly present in the lower 10% of the troposphere, and so these 10^{20} fragments exist in an atmosphere volume $1/10^{\text{th}}$ of that used in the Caesar paradigm, i.e. 10^{21} tidal volumes. Thus, we find *on average* that one SARS-CoV-2 fragment will be inhaled by each uninfected individual on Earth every ten breaths. Humans take ca 1.5×10^4 tidal breaths per day. Over one month of the early epidemic each individual will have breathed ca 5×10^5 times, inhaling on average ca 50,000 viral fragments. We re-stress that these are crude estimates, but they give us a sense of the orders of magnitude involved.

Appendix B: mathematical details

In this appendix we provide mathematical details of the incorporation of the PCF mechanism into the classic SIR model of epidemiology (Kermack and McKendrick 1927, Bailey 1975).

The SIR model

The SIR model tracks the dynamics of three subpopulations: susceptible, infected and recovered. It is convenient to normalise these subpopulations by the total population size, and to denote the density of subpopulations by s , i , and r respectively. The dynamics of the infection can be described by the following first-order differential equations:

$$\begin{aligned}\frac{ds}{dt} &= -\beta is \\ \frac{di}{dt} &= \beta is - \gamma i \\ \frac{dr}{dt} &= \gamma i\end{aligned}$$

where β is the rate of infection given contact between a susceptible and an infected individual and γ is the rate of recovery and/or death (these two outcomes are aggregated in this simplest model, as the “recovered” compartment is an absorbing state and plays no further role in the dynamics).

This model shows first an exponential increase in the number of infected individuals, and then, as the number of susceptible individuals decreases there comes a tipping point at which the rate of production of new infected individuals is less than the loss of infected individuals through “recovery”. Then the number of infected individuals rapidly vanishes and the resulting population will be a mixture of recovered and susceptible. The conventional concept of herd immunity is thereby implicit in this simple model.

Incorporating the PCF into the SIR model

We retain here the minimal model assumption of a completely mixed population, in order to see most clearly the effects of adding the PCF. A new subpopulation P is identified, that being pre-conditioned individuals, the density of which is denoted by p . In addition, we denote the strength of the PCF by the function φ . The SIR model equations above are extended to the following set:

$$\begin{aligned}\frac{ds}{dt} &= -\beta is - \alpha\varphi s + \epsilon p \\ \frac{di}{dt} &= \beta is - \gamma i \\ \frac{dr}{dt} &= \gamma i \\ \frac{dp}{dt} &= \alpha\varphi s - \epsilon p \\ \frac{d\varphi}{dt} &= \kappa i - \lambda\varphi\end{aligned}$$

In these equations, α is the rate at which a susceptible individual is pre-conditioned on exposure to the PCF, ε is the rate at which a pre-conditioned individual reverts to being susceptible, κ is the rate of production of the PCF by infected individuals, and λ is the PCF environmental degradation rate. We have retained the original SIR terms in black for clarity, and have written the additional PCF terms and equations in blue. These equations correspond to the schematic in Figure 1. These model equations, in the simple case of a non-spatial population, are relatively independent of any particular instantiation of the PCF. This mathematical form of extension of the SIR model may well exist in the vast epidemiology literature, possibly arising from a concept other than the PCF, given the innumerable extensions that have been made to the SIR model over the years. The author has not found any such examples to date.

We have used numerical integration with a basic 2nd order Runge-Kutta algorithm (Press et al 1992) to solve these equations for various combinations of parameter values. This provides a more detailed understanding of the possible dynamical outcomes of the PCF (see section 3). For the parameter values used, a time increment of 10^{-3} has been sufficient to ensure accuracy of the solutions. In section 3 and Figure 4 we refer to the “epidemic curve”, which we define here to be the rate of newly recovered individuals over time. We denote this $q(t)$ and it is equal in value to $dr/dt = \gamma i$. The code used for this numerical work is provided in the Supplementary Information as a separate file.

Important extensions of this basic model include population structure (as discussed in the main text), and also the effects of stochasticity, to allow a connection to individual-based models, and the possibility of non-trivial effects induced by demographic stochasticity (McKane and Newman 2004, 2005). Continuum models including spatial degrees of freedom will allow connections to be made to partial differential equations, and the vast literature on pattern formation and travelling waves. There have been studies in the epidemiology literature of integro-differential equations arising from the SIR model with non-local processes (Wang and Wu 2010) and one can envisage that the SIR/PCF model presented here would result in similar equations after integrating out the mediating PCF φ .

Short-time analysis

We briefly present below some preliminary mathematical analysis of these equations for the simplified case of no reversion ($\varepsilon = 0$). An early-time analysis provides a guide on the required magnitudes of κ (the rate of PCF generation) and α (the rate of pre-conditioning) in order for the PCF mechanism to be effective in suppressing the epidemic.

We normalise the total population size to unity and as an initial condition seed an arbitrarily small infectious subpopulation: $i(0) = i_0 \ll 1$. Then $s(0) = 1 - i_0$ and $p(0) = \varphi(0) = r(0) = 0$. We will focus on the initial stages of the epidemic such that the susceptible population does not deviate appreciably from its initial value of approximately 1. This approximation is accurate for times such that $(\beta - \gamma)t \ll \ln(1/i_0)$. In this case we have:

$$\frac{di}{dt} \approx (\beta - \gamma)i$$

$$\frac{dr}{dt} = \gamma i$$

$$\frac{dp}{dt} \approx \alpha \varphi$$

$$\frac{d\varphi}{dt} = \kappa i - \lambda \varphi$$

It is straightforward to integrate these linearised equations, and we find

$$\begin{aligned}
 i(t) &\approx i_0 e^{(\beta-\gamma)t} \\
 r(t) &\approx \frac{i_0 \gamma}{(\beta-\gamma)} (e^{(\beta-\gamma)t} - 1) \\
 p(t) &\approx \frac{\alpha \kappa i_0}{(\beta-\gamma+\lambda)} \left[\frac{(e^{(\beta-\gamma)t} - 1)}{(\beta-\gamma)} - \frac{(1 - e^{-\lambda t})}{\lambda} \right]
 \end{aligned}$$

Comparing the exponential growth terms in these solutions we see that, *roughly speaking*, the pre-conditioned population will dominate the sum of the infected and recovered populations so long as $\alpha \kappa > \beta(\beta - \gamma + \lambda)$. Improving on this condition is not straightforward due to the non-linear behaviour of the equations. We find from numerical integration that the condition is in fact too stringent on the rates of pre-conditioning.

A more detailed analysis is required to explore, mathematically, the range of epidemic dynamics in the presence of the PCF, but is beyond the scope of this paper.

References

- Bailey NTJ 1975 *The mathematical theory of infectious diseases and its applications* 2nd ed. (Hafner Press, New York)
- Ballerini M et al 2008 *Interaction ruling animal collective behavior depends on topological rather than metric distance: evidence from a field study* PNAS **105** 1232-1237
- Bar-On YM, Flamholz A, Phillips R, Milo R 2020 *SARS-CoV-2 (COVID-19) by the numbers* eLife **9** 357309
- Bedford T, Cobey S, Beerli P, Pascual M 2010 *Global migration dynamics underlie evolution and persistence of human influenza A (H3N2)* PLoS Path. **6** 1000918
- Benn CS, Netea MG, Selin LK, Aaby P 2013 *A small jab – a big effect: nonspecific immunomodulation by vaccines* Trends in Immunology **34** 431-439
- Berryman AA, Hawkins BA, Hawkins BA 2006 *The refuge as an integrating concept in ecology and evolution* OIKOS **115** 192-196
- Chang L, Tsai D 2017 *The code for facial identity in the primate brain* Cell **169** 1013–1028
- Chowell G, Sattenspiel L, Bansal S, Viboud C 2016 *Mathematical models to characterize early epidemic growth: a review* Phys. Life Rev. **18** 66-97
- Darwin CR 1859 *On the origin of species by means of natural selection* (John Murray, London)
- Després VR, et al 2012 *Primary biological aerosol particles in the atmosphere: a review* Chem. Phys. Meteorology **64** 15598
- Dillon MB, Dillon CF 2020 *Particle based model for airborne disease transmission* medRxiv, doi: 10.1101/2020.04.23.20076273
- Friston KJ et al 2020 *Dynamic causal modelling of COVID-19* (preprint, arXiv:2004.04463)
- Gilbert SF 2003 *Developmental Biology* (Sinauer, Sunderland MA)
- Heesterbeek H et al 2015 *Modeling infectious disease dynamics in the complex landscape of global health* Science **347** 6227
- Ianni A, Rossi N 2020 *Describing the COVID-19 outbreak fitting modified SIR models to data* medRxiv, doi: 10.1101/2020.04.29.20084285
- Kenah E, Chao DL, Matrajt L, Halloran ME, Longini IM 2011 *The Global Transmission and Control of Influenza* PLoS One **6** e19515
- Kermack WO, McKendrick AG 1927 *Contributions to the mathematical theory of epidemics (part 1)* Proc. Roy. Soc. Edinburgh A Math. **115** 700–721.
- Kleinnijenhuis J et al 2012 *Bacille Calmette-Guérin induces NOD2-dependent nonspecific protection from reinfection via epigenetic reprogramming of monocytes* PNAS **109** 17537-17542
- Kraemer MUG et al 2020 *The effect of human mobility and control measures on the COVID-19 epidemic in China* medRxiv, doi: 10.1101/2020.03.02.20026708
- Kucharski AJ 2020 *Early dynamics of transmission and control of COVID-19: a mathematical modelling study* Lancet Inf. Dis. **20** 553-58
- Lewis K 2007 *Persister cells, dormancy and infectious disease* Nature Rev **5** 48-56
- Lourenço J et al 2020 *Fundamental principles of epidemic spread highlight the immediate need for large-scale serological surveys to assess the stage of the SARS-CoV-2 epidemic* medRxiv, doi: 10.1101/2020.03.24.20042291
- Mayr E 2001 *What evolution is* (Basic Books, New York)
- McDonough A, Weinstein JR 2016 *Neuroimmune response in ischemic preconditioning* Neurotherapeutics **13** 748–761
- McKane AJ and Newman TJ 2004 *Stochastic models in population biology and their deterministic analogs* Phys. Rev. E **70** 041902
- McKane AJ and Newman TJ 2005 *Predator-prey cycles from resonant amplification of demographic stochasticity* Phys. Rev. Lett. **94** 218102

- Moran RJ et al 2020 *Estimating required 'lockdown' cycles before immunity to SARS-CoV-2: model-based analyses of susceptible population sizes, 'S0', in seven European countries including the UK and Ireland* medRxiv, doi: 10.1101/2020.04.10.20060426
- Newman TJ, Antonovics J, Wilbur HM 2002 *Population dynamics with a refuge: fractal basins and the suppression of chaos* Theor. Pop. Biol. **62** 121-128.
- O'Sullivan D, Gahegan M, Exeter DJ, Adams B 2020 *Spatially explicit models for exploring COVID-19 lockdown strategies* Trans GIS **00** 1-34
- Parrish JK, Viscido SV, Grünbaum D 2002 *Self-organized fish schools: an examination of emergent properties* Biol. Bull. **202** 296-305
- Press WH, Teukolsky SA, Vetterling WT, Flannery BP 1992 *Numerical recipes in Fortran: the art of scientific computing* 2nd ed (Cambridge University Press, Cambridge)
- Saladin KS 2007 *Anatomy and Physiology* 4th ed (McGraw-Hill, New York)
- Sallusto F, Lanzavecchia A, Araki K, Ahmed R 2010 *From vaccines to memory and back* Immunity **33** 451-63
- Sereina H et al 2020 *Seroprevalence of IgG antibodies against SARS coronavirus 2 in Belgium – a prospective cross-sectional study of residual samples* medRxiv, doi: 10.1101/2020.06.08.20125179
- Sheldrake R 2009 *A new science of life* (Icon Books, London)
- Strassmann J, Queller DC 2011 *How social evolution theory impacts our understanding of development in the social amoeba Dictyostelium* Devel. Growth Differ. **53** 597–607
- Streeck et al 2020 *Infection fatality rate of SARS-CoV-2 infection in a German community with a super-spreading event* medRxiv, doi: 10.1101/2020.05.04.20090076
- Tinsley JN et al 2016 *Direct detection of a single photon by humans* Nat. Comm. **7** 12172
- Turing A 1952 *The chemical basis of morphogenesis*, Phil. Trans. Roy. Soc. Lon. B **237** 37-72
- Verity R et al. 2020 *Estimates of the severity of coronavirus disease 2019: a model-based analysis* Lancet Inf. Dis. **20** 669-77
- Viboud C, Bjørnstad ON, Smith DL, Simonsen L, Miller MA, Grenfell BT 2006 *Synchrony, waves, and spatial hierarchies in the spread of influenza* Science **312** 447-451
- Wang Z-C, Wu J 2010 *Travelling waves of a diffusive Kermack–McKendrick epidemic model with non-local delayed transmission* Proc. Roy. Soc. A **466** 237-261
- Wilson EO 1975 *Sociobiology: the new synthesis* (Harvard University Press, Cambridge MA)
- Wilson EO, Hölldobler BK 1990 *The ants* (Harvard University Press, Cambridge MA)
- Wu F et al 2020 *Neutralizing antibody responses to SARS-CoV-2 in a COVID-19 recovered patient cohort and their implications* medRxiv, doi: 10.1101/2020.03.30.20047365
- Wu JT, Leung K, Leung GM 2020 *Nowcasting and forecasting the potential domestic and international spread of the 2019-nCoV outbreak originating in Wuhan, China: a modelling study* Lancet **395** 689-697
- Zhu N et al 2020 *A novel coronavirus from patients with pneumonia in China, 2019* New Eng. J. Med. **382** 727-733

www.youtube.com/watch?v=uk2YZfnsOPg

[Karol Sikora interviewed by Freddie Sayers of Unherd]

www.worldometers.info/coronavirus

[Internationally sourced datasets of COVID-19 incidence and mortality for all affected countries, updated daily]

www.ons.gov.uk

[weekly figures for COVID-19 deaths in England and Wales, incl. data on gender and age]

Significant efforts have been made to cite epidemiological, immunological and biophysical studies having a direct bearing on the PCF concept. Given the diverse subject areas contributing to the PCF hypothesis, comprehensiveness of surveying the literature has been balanced against the imperative of making results public in a timely fashion, to inform ongoing efforts to combat the COVID-19 pandemic. References will be updated as appropriate based on feedback.

Acknowledgements

The author is sincerely grateful to Rupert Sheldrake for helpful discussions and comments on the manuscript.

Short biography

Thea Newman has thirty years' experience in scientific research and has held academic positions at the University of Virginia (2000-2002), Arizona State University (2002-2010) and the University of Dundee (2011-2017). Her training is originally in theoretical physics. Since 2000 she has pursued theoretical biophysics research across a range of biological areas: ecology, developmental biology, molecular biology and most recently cancer. Since 2018 she has directed SOLARAVUS, working as an independent educator and researcher.

Thea Newman is not an expert *per se* in immunology, epidemiology or atmospheric science. This paper is offered to the public and the scientific community in the form of a theoretical hypothesis supported by preliminary analysis. It is hoped to be of utility in better understanding and managing the COVID-19 pandemic and subsequent epidemics.

List of acronyms

COVID-19	coronavirus disease 2019, caused by the SARS-CoV-2 virus
PCF	pre-conditioning field
SIR	susceptible-infected-recovered (epidemiological model)
STP	standard temperature and pressure
ViDe	viral detritus

Supplementary information

The computer code used to integrate the mathematical equations in Appendix B is provided as an additional file 'PCF.f90' on the SOLARAVUS website. The code has been kept as simple as possible, using a 2nd order Runge-Kutta integrator. It is written in Fortran 90, commented for ease of interpretation, and can be used on any platform for which a Fortran compiler is available.

Figures

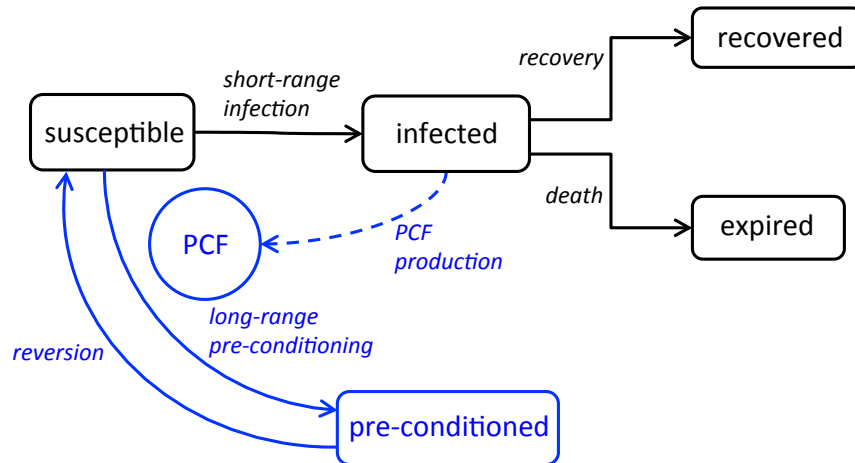


Figure 1: schematic diagram illustrating the concept of pre-conditioning. Black boxes and labels describe the classic SIR model of epidemiology. Blue boxes and labels describe in the simplest form the emergent pre-conditioning mechanism mediated by the PCF.

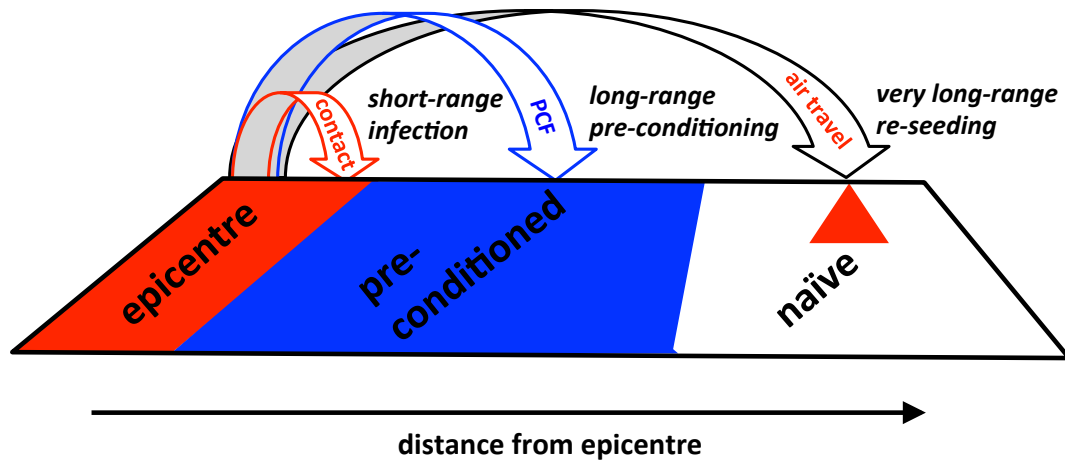


Figure 2: schematic diagram illustrating spatial dynamics of PCF. The original epicentre has no pre-conditioning and high rates of infection through local contact. The emerging PCF is longer ranged and allows pre-conditioning of more distant populations over time, leading to lower infection and mortality rates as the epidemic spreads. New epicentres of infection can be established in very distant “naïve populations”, which have yet to experience infection or pre-conditioning, but which are accessible to the pathogen through intercontinental air travel of infected individuals.

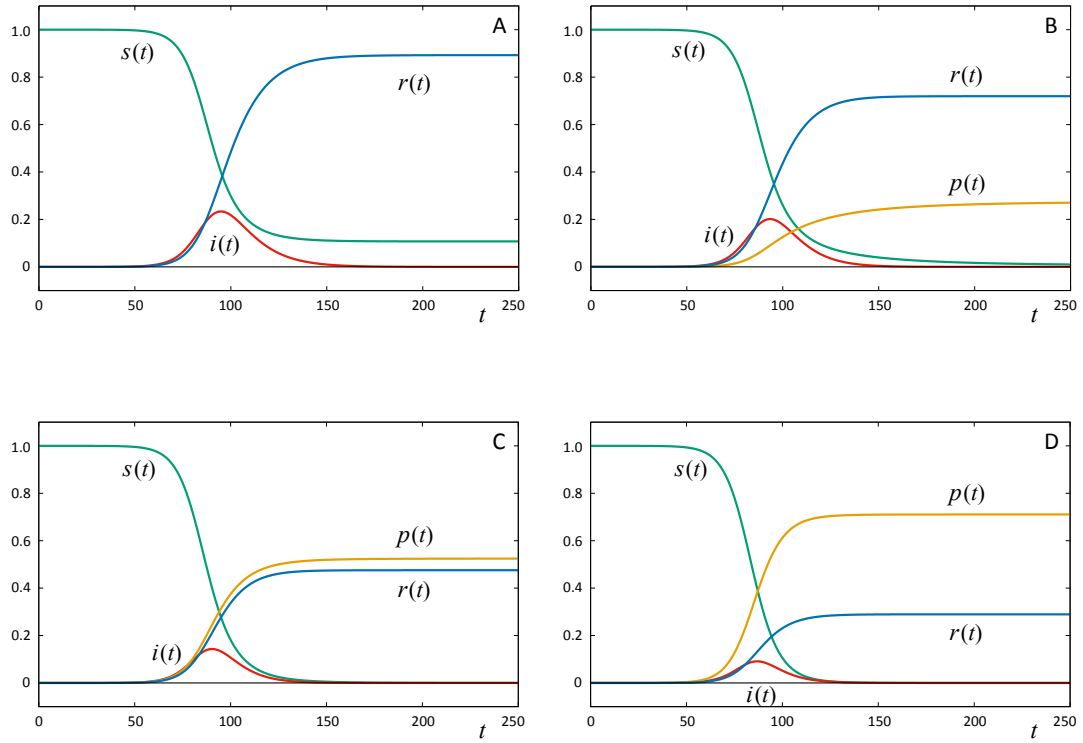


Figure 3: Numerical integration of the SIR model with the additional PCF mechanism, in the form of the boxed differential equations in Appendix B. Panels show the densities of the subpopulations as a function of time, with susceptible, infected, recovered and pre-conditioned population trajectories in green, red, blue and orange respectively. The reversion process is absent here, i.e. $\varepsilon = 0$. The total population density is normalised to unity. The initial condition is $i(0) = i_0$, $s(0) = 1 - i_0$ with $i_0 = 10^{-6}$, and all other densities initialised to zero. The time increment used is 10^{-3} . The rate parameters are set to $\beta = 0.25$, $\gamma = 0.1$, $\kappa = 1.0$, $\lambda = 0.01$. The strength of the pre-conditioning process is increased from zero (absence of preconditioning) through panels A to D, with values $\alpha = 0.0, 0.005, 0.02, 0.05$ respectively. Note the increasing suppression of the infection and recovered compartments, and the increasing buffering of the population (occupying the pre-conditioned compartment) as α is increased.

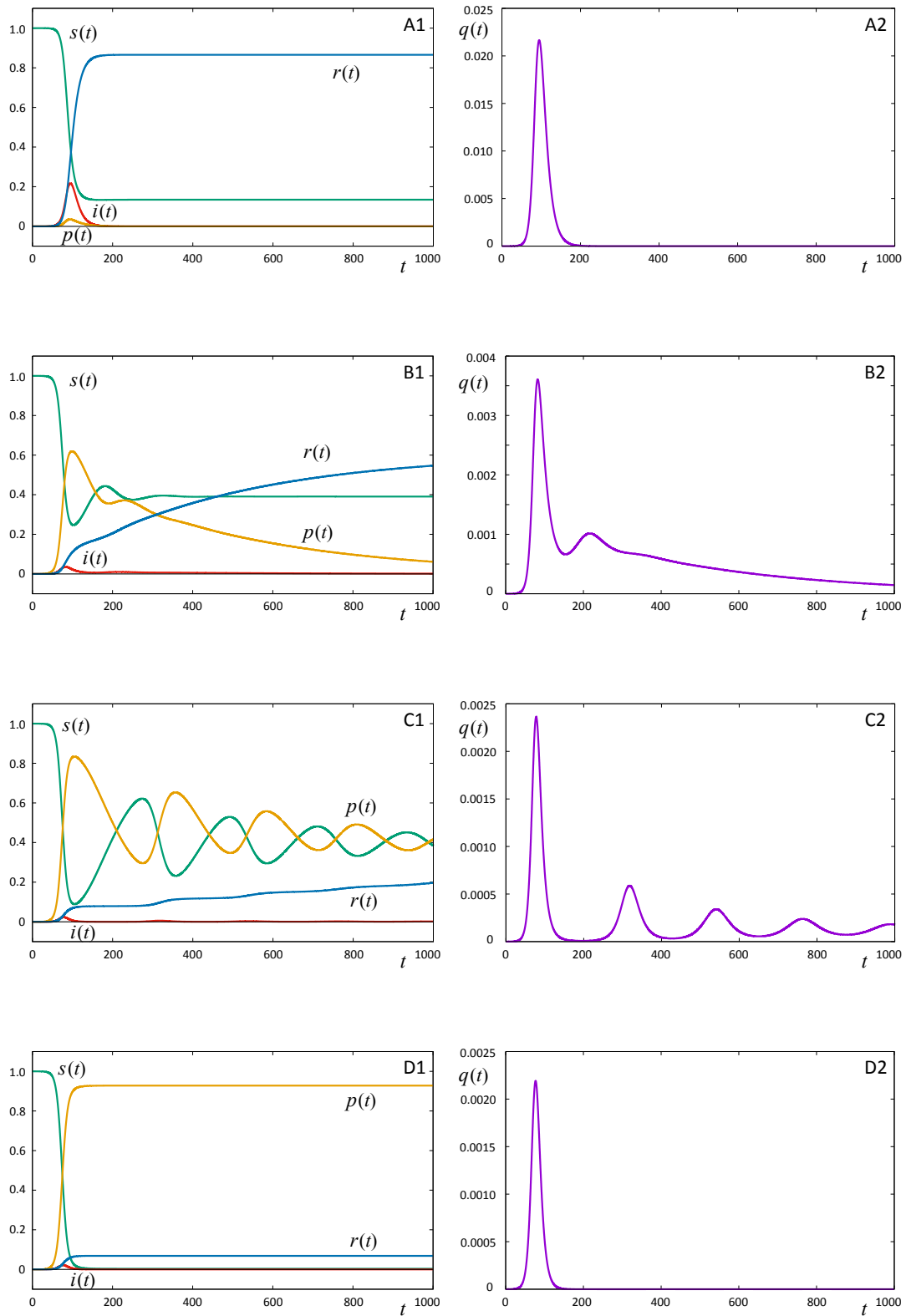


Figure 4: Numerical integration of the SIR model with the additional PCF mechanism, in the form of the boxed differential equations in Appendix B. The reversion process is now present, i.e. $\varepsilon \neq 0$ (except in panels D1 and D2 which show the control with no reversion). Panels on the left show the densities of the subpopulations as a function of time, with

susceptible, infected, recovered and pre-conditioned population trajectories in green, red, blue and orange respectively. Partner panels on the right are for the same parameter values and show $q(t)$, the rate of increase in recovered individuals, which is used as a measure of the epidemic curve. As before the total population density is normalised to unity. The initial condition is $i(0) = i_0$, $s(0) = 1 - i_0$ with $i_0 = 10^{-6}$, and all other densities initialised to zero. The time increment used is 10^{-3} . The rate parameters are set to $\alpha = 0.4$, $\beta = 0.25$, $\gamma = 0.1$, $\kappa = 1.0$, $\lambda = 0.05$. The rate of reversion has the values $\varepsilon = 10.0, 0.08, 0.01, 0.0$ through panels A to D. Note that an extremely high rate of reversion (A panels) effectively removes the efficacy of the PCF buffering, as expected. As the reversion rate is decreased (B panels) the buffering becomes effective, though dynamic, and the right tail of the epidemic curve broadens considerably creating the so-called “heavy tail”. Further decreasing the reversion rate leads to clearly separated waves of epidemic (C panels). In the absence of reversion (D panels) the buffering is strongly dominant, consistent with the results shown in Figure 3, and the epidemic curve loses the “heavy tail” feature.